

## A Color Appearance Model Applicable in Mesopic Vision

JaeChul SHIN, Naoki MATSUKI, Hirohisa YAGUCHI<sup>1</sup> and Satoshi SHIOIRI<sup>1</sup>

*Graduate School of Science and Technology, Chiba University, 1-33 Yoyoicho, Inage-ku, Chiba 263-8522, Japan*

<sup>1</sup>*Department of Information and Image Sciences, Chiba University, 1-33 Yoyoicho, Inage-ku, Chiba 263-8522, Japan*

(Received October 30, 2003; Accepted January 29, 2004)

We propose a color vision model that can be used to predict color appearance in mesopic vision as well as photopic and scotopic vision. It is based on a two-stage model which consists of the cone and opponent stages and it assumes rod intrusion at the opponent stage. The model has the following features to describe the color appearance in mesopic vision. First, it includes a gradual and nonlinear shift in spectral luminous efficiency from  $V(\lambda)$  to  $V'(\lambda)$  to cope with the spectral sensitivity difference between photopic and scotopic vision and the nonlinearity of rod influence on the luminance channel. Second, the model assumes decrease of the chromatic component with decreasing illuminance to explain the reduction of saturation at low illuminance levels. Third, it assumes that red/green and yellow/blue components change with illuminance levels independently, thus explaining hue shifts with decreasing illuminance. We applied the model for color appearance simulation of natural scenes in a mesopic visual environment.

**Key words:** mesopic vision, color appearance, color appearance modeling, opponent-color vision model, mesopic color reproduction

### 1. Introduction

A typical model of human color vision has two levels of processing, which copes with trichromatic theory and opponent theory. The outputs of three types of cones at the first stage are converted to three types of opponent signals at the second stage (the luminance channel and the red/green and yellow/blue color opponent channels). Based on such a two-stage model, many color vision models<sup>1–5)</sup> have been proposed considering properties of color vision psychophysically determined. However, most of them are models in photopic vision. If color vision in the evening or at night is of interest, a model has to consider the influence of rods on the color appearance. The rod intrusion to color vision is not simple and the details have not been understood. Color vision models proposed previously lack appropriate rod intrusion and cannot be applied to predict color appearance in mesopic vision.

There is one color appearance model, Hunt 94,<sup>6)</sup> that predicts color appearance for a wide range of illuminance levels, including mesopic and scotopic levels. The model has several parameters to control the amount of rod intrusion and the prediction performance is acceptable for many applications. However, the model requires complex calculations that are difficult to implement and the decision on the appropriate parameter values is not easy.<sup>7)</sup>

Buck *et al.*<sup>8)</sup> investigated model characteristics that can interpret the rod influence on color vision, adding rod intrusion to a couple of color models.<sup>3,4)</sup> They considered models that explain asymmetric rod contributions between hues. Asymmetric rod contribution is the phenomenon such that adding the rod signal to yellow shifts the hue toward green and adding the rod signals to blue shifts the hue toward red. In the models they considered, rod signal intrudes on each of the L, M and S cone outputs with a different amount of rod contribution depending on the channels. Although some of their experimental results suggest asymmetry of rod contribution, results of other studies suggest that rod contributes to red/green and yellow/blue opponent processes, which change the perceived hue.

Color appearance estimation of a wide variety of test colors is necessary to determine what types of processing in models characterize color vision with rod intrusion.

We investigated the color appearance of a variety of test colors in various illuminance levels and previously reported the results.<sup>9–11)</sup> The experiment was designed to collect data required for modeling color appearance in mesopic vision as well as photopic and scotopic vision. In the present study, we built a model based on the color appearance results measured in the previous experiment. Our model adds rod intrusion to the two-stage model proposed by Boynton.<sup>2)</sup> The model has rod intrusion both in the two color opponent channels and the luminance channel so that hue, saturation and lightness shift with illuminance levels. Model parameters are determined to predict the experimental results and the model performance is evaluated by color differences between the experimental data and prediction from the model.

### 2. Experimental Results

We built a model based on the color appearance measurements in our previous reports. The experiment measured the corresponding color of 48 color chips under various illuminance levels by an asymmetric color matching experiment. The appearance of each test color chip was matched by the observer adjusting color on a Cathode-Ray Tube (CRT) display under a photopic level of illuminance. We reported the results plotted on the CIELAB color space for not only chroma and lightness but hue of the most color chips changed with illuminance.<sup>11)</sup>

In order to compare the experimental results and prediction from the model, we used an opponent-color space in this study. This opponent-color space can presume the contributions and interactions of each cone for color vision mechanism. The color diagram in Fig. 1 corresponds to the outputs of the two-stage model proposed by Boynton. Although the model is simple, it can describe the many phenomena of color vision. The model assumes that the opponent process converts signals from L, M and S cones to red/green, yellow/blue opponent-color and luminance re-

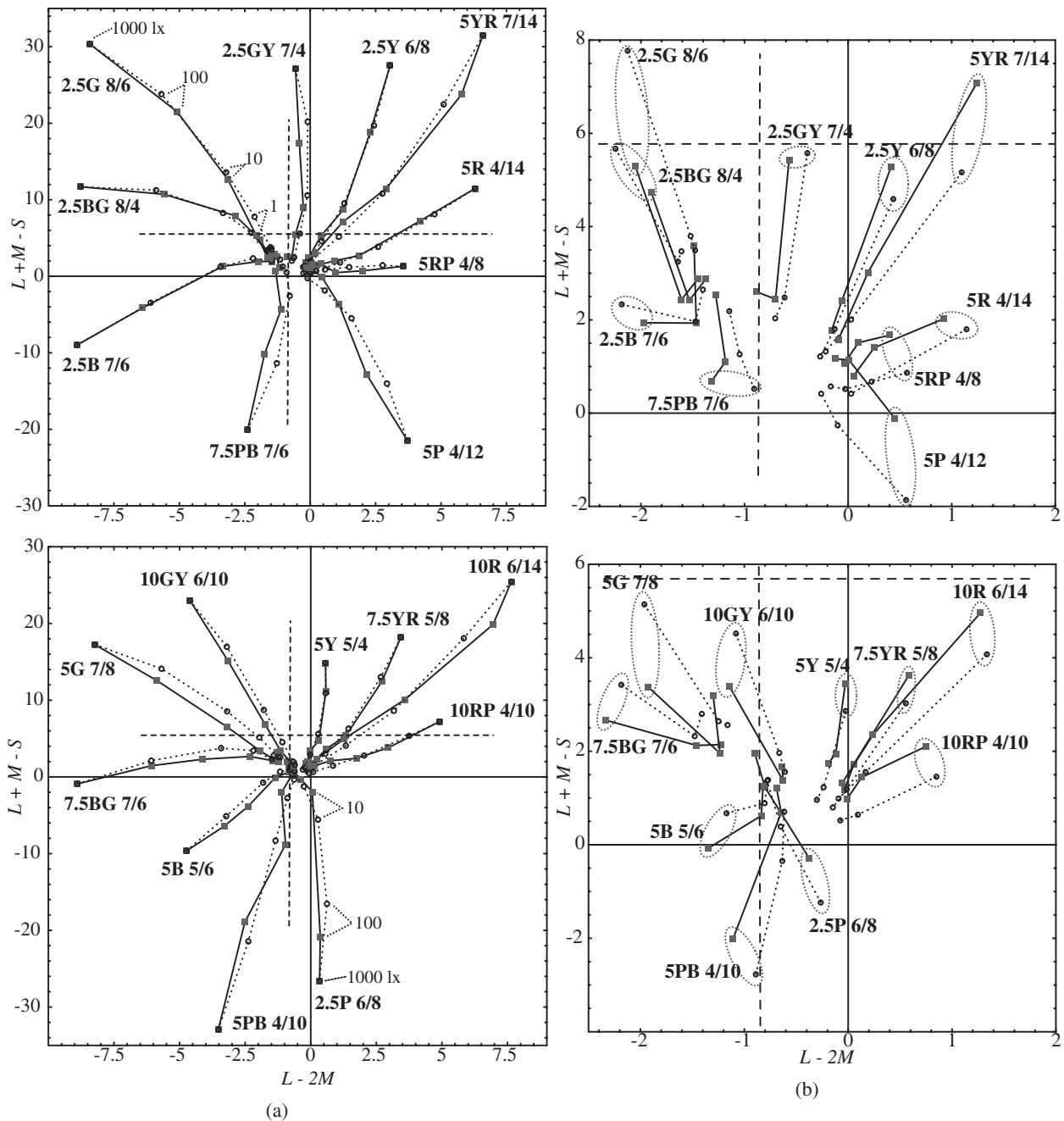


Fig. 1. Change of color appearance according to illuminance levels. Experimental values (solid lines) and predicted values (dotted lines) by the model are plotted together. (a) Data for all six illuminance levels. (b) Data for three darkest illuminance levels (1 ~ 0.01 lx). The intersection of two dashed lines indicates the actual matching point for N5 under 1000 lx.

sponses, that is,  $L - 2M$ ,  $L + M - S$  and  $L + M$ , respectively. Before the conversion, the spectral responses of the three cones,  $L$ ,  $M$  and  $S$  were derived using the Judd modified color matching functions ( $\bar{x}'(\lambda)$ ), ( $\bar{y}'(\lambda)$ ) and ( $\bar{z}'(\lambda)$ ), following Smith and Pokorny,<sup>12)</sup> as shown in eqs. (1) and (2):

$$\begin{pmatrix} L \\ M \\ S \end{pmatrix} = \begin{pmatrix} 0.15514 & 0.54312 & -0.03286 \\ -0.15514 & 0.45684 & 0.03286 \\ 0 & 0 & 1.00000 \end{pmatrix} \begin{pmatrix} X_{\text{Judd}} \\ Y_{\text{Judd}} \\ Z_{\text{Judd}} \end{pmatrix} \quad (1)$$

where  $X_{\text{Judd}}$ ,  $Y_{\text{Judd}}$  and  $Z_{\text{Judd}}$  are the Judd modified XYZ tristimulus values, which are given in eq. (2).

$$\begin{aligned} X_{\text{Judd}} &= k \int P(\lambda) \bar{x}'(\lambda) d\lambda \\ Y_{\text{Judd}} &= k \int P(\lambda) \bar{y}'(\lambda) d\lambda \end{aligned} \quad (2)$$

$$\begin{aligned} Z_{\text{Judd}} &= k \int P(\lambda) \bar{z}'(\lambda) d\lambda \\ k &= 100 / \int P_w(\lambda) \bar{y}'(\lambda) d\lambda \end{aligned} \quad (3)$$

The coefficient,  $k$  is a unit for normalizing the  $Y_{\text{judd}}$  value to white. If the spectral radiance of white of a CRT display is given as  $P_w(\lambda)$ , then  $P_w(\lambda) = r(\lambda) + g(\lambda) + b(\lambda)$  where  $r(\lambda)$ ,  $g(\lambda)$  and  $b(\lambda)$  indicate the spectral radiance at the maximum luminance of each primary of a CRT display. Similarly, the spectral radiance of a given stimulus on the CRT display,  $P(\lambda)$ , is calculated as follows,

$$P(\lambda) = \frac{R}{R_w} r(\lambda) + \frac{G}{G_w} g(\lambda) + \frac{B}{B_w} b(\lambda) \quad (4)$$

where  $R$ ,  $G$  and  $B$  are the tristimulus value of the color on a CRT display, and  $R_w$ ,  $G_w$  and  $B_w$  are the tristimulus values of each primary component for the white on the CRT display.

Figure 1(a) shows the experimental results in the opponent color space  $L - 2M$  and  $L + M - S$  plane, describing changes of corresponding color of test color chips for six illuminance levels (1000, 100, 10, 1, 0.1, and 0.01). The symbols with solid lines represent experimental values and those with dotted lines represent predicted values by the model mentioned later (see section 3.2). The 20 chips selected from 48 test chips are shown in Fig. 1(a), using two panels for clarity. The chips are chosen to be approximately equally spaced in hue angle. Figure 1(b) shows the results of the darkest three illuminance levels (1, 0.1 and 0.01 lx) to show the detail of the central area in Fig. 1(a). Figure 2 shows the change of  $L + M$  value, which corresponds to the luminance factor of the experimental value (solid lines) and predicted values (dotted lines). The value of  $L + M$  here is not absolute luminance, but a value normalized so that white has a value of 100. That is, the luminance of matching color for a test chip was divided by that for the white with a maximum luminance on the CRT. Figure 3 shows the relationship between the photopic and scotopic luminance factors. The vertical axis indicates the photopic luminance factor of corresponding color which appears equal in brightness to the test chip at 0.01 lx, and the horizontal axis indicates the scotopic luminance factor of each test chip. The relationship is nonlinear and is expressed by a power function.

We summarize the experimental results as follows. First, the chromatic component (saturation) of test colors decreases with decrease in illuminance. Since the decrease of chromatic component occurs both at high illuminances (above 10 lx) and at low illuminances (below 1 lx), perhaps both cones and rods influence the changes in this component. Second, hue changes with decrease in illuminance. The loci of corresponding colors bend in a peculiar way for each hue. The loci indicate hue shift even with consideration of the Abney hue shift, which is hue change with saturation or colorimetric purity. The loci of yellowish, reddish and purplish chips bend toward the reddish direction with decrease in illuminance level above 1 lx, below which level the loci are relatively straight. The loci of bluish chips bend toward the greenish direction with decrease in illuminance level above 1 lx, below which level the loci are relatively straight. Third, color is perceived even at the illuminance of 0.01 lx. The coordinates of corresponding colors at this level distribute with two peaks (bimodal distribution). The

coordinates of the distribution center suggest that reddish test colors appear to be slightly more reddish (larger values in  $L - 2M$ ) than the others and most of the test colors appear to be bluish (smaller values in  $L + M - S$  than neutral gray, the intersection of the dashed lines). Fourth, lightness decreases with decrease in illuminance level throughout the illuminance levels for all test chips except bluish chips, for which lightness does not decrease and even increases in some cases below 10 lx. The model proposed in the present study explains these features.

### 3. A Mesopic Color Appearance Model

#### 3.1 Outline of the model

The present model modifies the Boynton's two-stage color-vision model, in which the red/green and yellow/blue opponent channels and the luminance channels are represented by equations  $L - 2M$ ,  $L + M - S$  and  $L + M$ . The presented model puts a rod intrusion in each of the opponent channels and rod signals and their amount varied depending on the illuminance levels and on the channels. The amount of the cone signals also varied depending on the illuminance levels and on the channels. The weight of cone signals decreases with decrease in illuminance while the weight of rod signals increase. The output of each channel is formulated in eqs. (5), (6) and (7),

$$A(E) = \alpha(E)K_w((L_p + M_p)/(L_p + M_p)_w) + \beta(E)K'_w(Y'/Y'_w)^\gamma \quad (5)$$

$$r/g(E) = l(E)(L_p - 2M_p) + a(E)Y' \quad (6)$$

$$b/y(E) = m(E)(L_p + M_p - S_p) + b(E)Y' \quad (7)$$

where  $L_p$ ,  $M_p$  and  $S_p$  represent cone outputs at photopic condition, and  $A(E)$ ,  $r/g(E)$  and  $b/y(E)$  represent outputs of the luminance, red-green and blue-yellow channels at illuminance level of  $E$ .  $Y'$  represents the scotopic luminance factor, which can be regarded as rod output.  $Y'$  is calculated for each test chip by the CIE spectral luminous efficiency  $V'(\lambda)$  and normalized by white as shown in eq. (8),

$$Y' = k' \int R(\lambda)I(\lambda)V'(\lambda)d\lambda \quad (8)$$

where

$$k' = 100 \int I(\lambda)V'(\lambda)d\lambda$$

$R(\lambda)$  and  $I(\lambda)$  indicate the spectral reflectance of the test chip and the spectral irradiance on this chip. A quota,  $k'$ , was determined to be  $Y'$  equal to 100 for reference white.  $(L_p + M_p)_w$  and  $Y'_w$  are outputs of photopic and scotopic luminance channels for white. The weighting coefficients,  $\alpha(E)$  and  $\beta(E)$  indicate contribution amounts of photopic and scotopic luminance as a function of illuminance  $E$ .  $K_w$  and  $K'_w$  indicate the maximum response (the response to white) of the luminance channel at photopic and scotopic levels, and  $\gamma$  is the parameter to express the nonlinear relationship between photopic and scotopic luminance channels. The weighting coefficients,  $l(E)$  and  $a(E)$  indicate contribution amounts of the photopic red/green process (red/green signal made of L and M cone outputs) and rod to the red/green

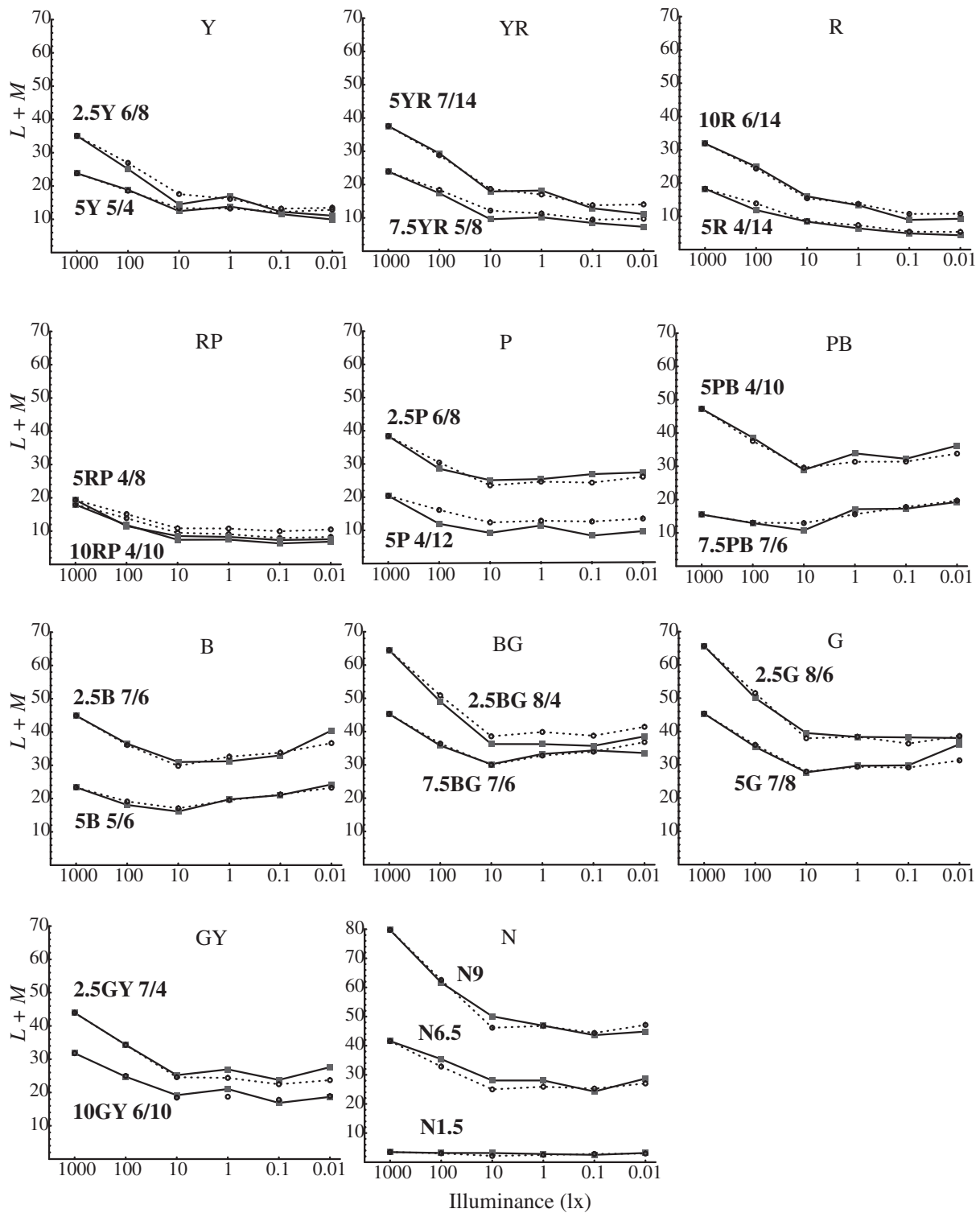


Fig. 2. Change of perceived luminance as a function of illuminance. Experimental values (solid lines) and predicted values (dotted line) by the model are plotted together for 20 chromatic test chips and three neutral color test chips.

channel. The weighting coefficients,  $m(E)$  and  $b(E)$  indicate contribution amounts of the photopic yellow/blue process (yellow/blue signal made of L, M and S cone outputs) and rod to the yellow/blue channel. These weighting coefficients vary with illuminance level of  $E$  to express the change of contribution amounts of the factors among different illuminance levels.

The model is designed to predict the features of the experimental results. To explain the first feature, the decrease in chromatic component of test colors with decrease in illuminance, the contribution amounts of the photopic color opponent channels (the coefficients,  $l(E)$  and  $m(E)$ ) decrease with decrease in illuminance. To explain the second feature, the hue changes with illuminance levels, the

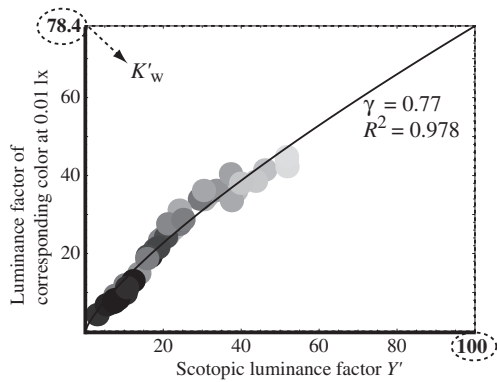


Fig. 3. Relationship between the scotopic luminance factor  $Y'$  and the luminance factor of corresponding color at 0.01 lx for each test chip.

model uses different functions of the change in contribution amounts of the photopic red/green and yellow/blue processes with illuminance levels. When reduction of the red/green output is larger than that of the yellow/blue one, hues shift toward ( $L - 2M$ )-axis. To explain the third feature, color perception at the illuminance of 0.01 lx, rod outputs contribute to the color opponent channels to activate color signals by some amount. To explain the fourth feature, the lightness change with illuminance level, contribution amount of the photopic luminance factor decrease and that of the scotopic luminance factor increase with decrease in illuminance level.

We obtain model parameters so that the model predicts the experimental results best by a least square method except for  $K_w$ ,  $K'_w$  and  $\gamma$ . The parameters,  $K_w$  and  $K'_w$  normalize luminance factors so that the factor of white becomes 100 at photopic illuminances and a value estimated from the experiment at scotopic illuminances. The values of 100 and 78.4 for  $K_w$  and  $K'_w$  reach the criteria. The value of  $K'_w$  is obtained from a function that approximates the relationship between the photopic and scotopic luminance factors. Figure 3 shows the normalized luminance factor of correspondence color to each test chip against the scotopic luminance factor of the test chip. The solid curve indicates a power function with an exponent ( $\gamma = 0.77$ ) for the least squares fitting to the data.

Weighting coefficients,  $\alpha(E)$ ,  $\beta(E)$ ,  $l(E)$ ,  $m(E)$ ,  $a(E)$  and  $b(E)$  are functions of illuminance  $E$ . The values were determined to predict the experimental results best at each illuminance level and are shown in Fig. 4 and in Table 1. The result of the parameters  $\alpha(E)$  and  $\beta(E)$  indicate that the influence of photopic and scotopic luminance factors change the amount gradually with illuminance level. Amount of the influence is about the same between 10 and 1 lx. With the weighting coefficient,  $l(E)$  and  $m(E)$ , the contribution amount of cone signals decreases with decrease in illuminance level, while with the weighting coefficient,  $a(E)$  and  $b(E)$ , the contribution amount of rod signals changes only slightly.

### 3.2 Performance of the model

Figure 1 and 2 reveal that the model reflects the basic

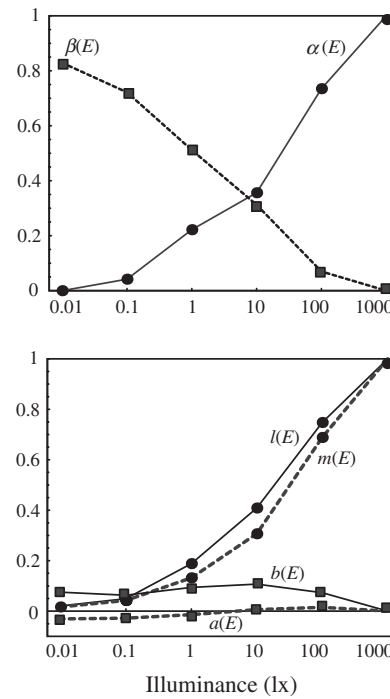


Fig. 4. Change of weighting coefficients of the model with illuminance level.

Table 1. Weighting coefficients of the model with illuminance level.

Weighting Coefficient	Illuminance (lx)					
	0.01	0.1	1	10	100	1000
$\alpha(E)$	0	0.042	0.222	0.356	0.735	1
$\beta(E)$	0.829	0.722	0.512	0.312	0.070	0
$l(E)$	0.020	0.049	0.188	0.409	0.748	1
$m(E)$	0.017	0.042	0.132	0.307	0.689	1
$a(E)$	-0.033	-0.028	-0.014	0.006	0.015	0
$b(E)$	0.075	0.063	0.094	0.107	0.073	0

features of the experimental results. Chromatic component decreases with decrease in illuminance, hue changes with decrease in illuminance similarly to the experimental results, color is perceived even at the illuminance of 0.01 lx and lightness changes differently for bluish and reddish chips as predicted from the Purkinje shift.

To estimate how accurately the model predicts the experimental results, we calculated the CIE color differences between the experimental data and model predictions obtaining  $L^*$ ,  $a^*$  and  $b^*$  coordinates using the Judd modified color matching functions. The 48 test color chips were grouped according to the Munsell hue notation (Y, YR, R...). The  $\Delta E_{ab}^*$ , the color difference of the CIELAB system is shown as a function of illuminance for each color category in Fig. 5. Although the color differences indicate the maximum value approximately at 10 lx, the average value is about 3 in the mesopic ranges (1 ~ 0.01 lx). This indicates that the model is applicable for simulating colors in mesopic vision for many practical purposes.

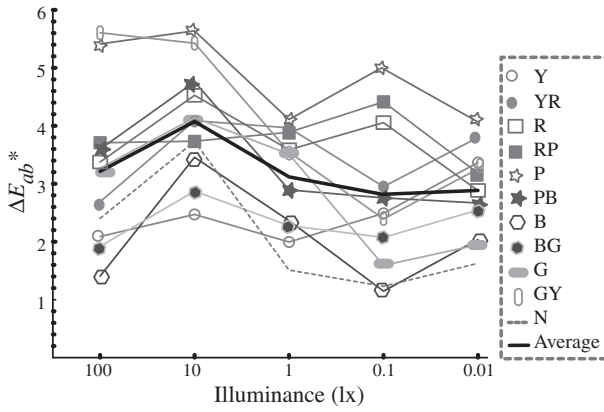


Fig. 5. The CIELAB color differences between predicted and experimental colors.

The qualitative estimation from Fig. 1(a) indicates that the error of the prediction is large for the purple region. The major error comes from the predictions of  $\Delta b^*$ . The  $\Delta b^*$  is the largest among  $\Delta L^*$ ,  $\Delta a^*$  and  $\Delta b^*$ , 2.01, 2.91 and 3.75, respectively, for the illuminance of 10 lx.

#### 4. Mesopic Color Reproduction

Figure 6 depicts a flow chart of model application to a scene from input to output. First, the scene of interest is digitized into a computer, with information of spectral distribution for each pixel,  $P_{ij}(\lambda)$ .  $P_{ij}(\lambda)$  is the product of the spectral reflectance  $R_{ij}(\lambda)$  and the spectral irradiance  $I(\lambda)$  of the illumination. Second, the pixel data are transformed to the Judd modified XYZ tristimulus values and the scotopic luminance factor,  $Y'$  using the eqs. (9) and (10),

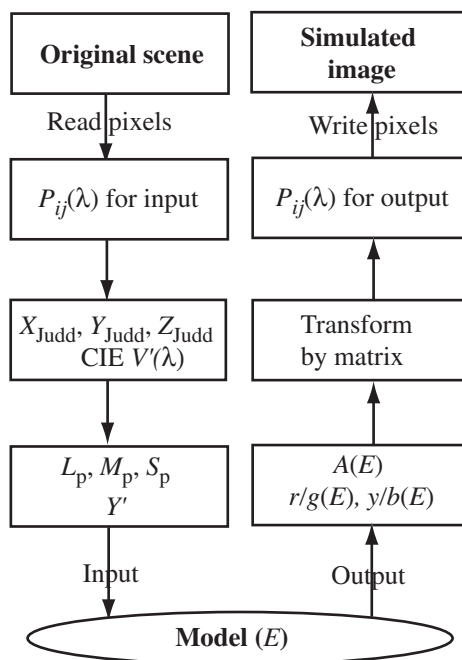


Fig. 6. Flow chart of the mesopic color reproduction.

$$X_{\text{Judd}} = k \int R_{ij}(\lambda) I(\lambda) \bar{x}'(\lambda) d\lambda$$

$$Y_{\text{Judd}} = k \int R_{ij}(\lambda) I(\lambda) \bar{y}'(\lambda) d\lambda \quad (9)$$

$$Z_{\text{Judd}} = k \int R_{ij}(\lambda) I(\lambda) \bar{z}'(\lambda) d\lambda$$

$$Y' = k' \int R_{ij}(\lambda) I(\lambda) V'(\lambda) d\lambda \quad (10)$$

where coefficients  $k$  and  $k'$  are the same as eqs. (2) and (8) and the subscript of  $ij$  indicates a pixel. Third, the Judd modified XYZ tristimulus values are converted to  $L_p$ ,  $M_p$  and  $S_p$  using eq. (1). Finally, to obtain output values of the opponent stage at a given illuminance  $E$ ,  $L_p$ ,  $M_p$  and  $S_p$  are input with the weighting coefficients,  $\alpha(E)$ ,  $\beta(E)$ ,  $l(E)$ ,  $m(E)$ ,  $a(E)$  and  $b(E)$ , to eqs. (5), (6) and (7). From the output, the tristimulus values of the CRT display which shows the simulated images can be easily calculated. From the output signals,  $A(E)$ ,  $r/g(E)$  and  $y/b(E)$ , the Judd modified XYZ tristimulus values are obtained as follows:

$$\begin{pmatrix} X_{\text{Judd}} \\ Y_{\text{Judd}} \\ Z_{\text{Judd}} \end{pmatrix} = \begin{pmatrix} 1.00802 & 2.14860 & -0.21181 \\ 1.00000 & 0 & 0 \\ 1.00000 & 0 & -1.00000 \end{pmatrix} \times \begin{pmatrix} A(E) \\ r/g(E) \\ y/b(E) \end{pmatrix} \quad (11)$$

Predicted color can be shown on a display transforming the Judd modified XYZ tristimulus values to the RGB tristimulus values of the CRT display.

Here, we describe the method and the results of simulation for a certain display. We use an image on a CRT display as the original and the spectral distribution of each pixel is determined. The reason we do not use an actual scene as the original is that it is difficult to obtain the spectral distribution for each point of the scene. For the image on the CRT display, spectral distribution of each pixel can be obtained from the spectral radiance of the red, green and blue phosphors as described in eq. (4). In this simulation, the chromaticities of red, green and blue phosphors of the CRT display are (0.624, 0.345), (0.280, 0.617) and (0.151, 0.078), respectively, in the Judd modified ( $x'$ ,  $y'$ ) coordinates. Equations (12) and (13) describe the relationship between the CRT display tristimulus values and the Judd modified XYZ tristimulus values:

$$\begin{pmatrix} X_{\text{Judd}} \\ Y_{\text{Judd}} \\ Z_{\text{Judd}} \end{pmatrix} = \begin{pmatrix} \frac{x'_r}{y'_r} & \frac{x'_g}{y'_g} & \frac{x'_b}{y'_b} \\ 1 & 1 & 1 \\ \frac{z'_r}{y'_r} & \frac{z'_g}{y'_g} & \frac{z'_b}{y'_b} \end{pmatrix} \begin{pmatrix} R \\ G \\ B \end{pmatrix} \\ = \begin{pmatrix} 1.80813 & 0.45398 & 1.94100 \\ 1 & 1 & 1 \\ 0.08763 & 0.16588 & 9.92330 \end{pmatrix} \begin{pmatrix} R \\ G \\ B \end{pmatrix} \quad (12)$$

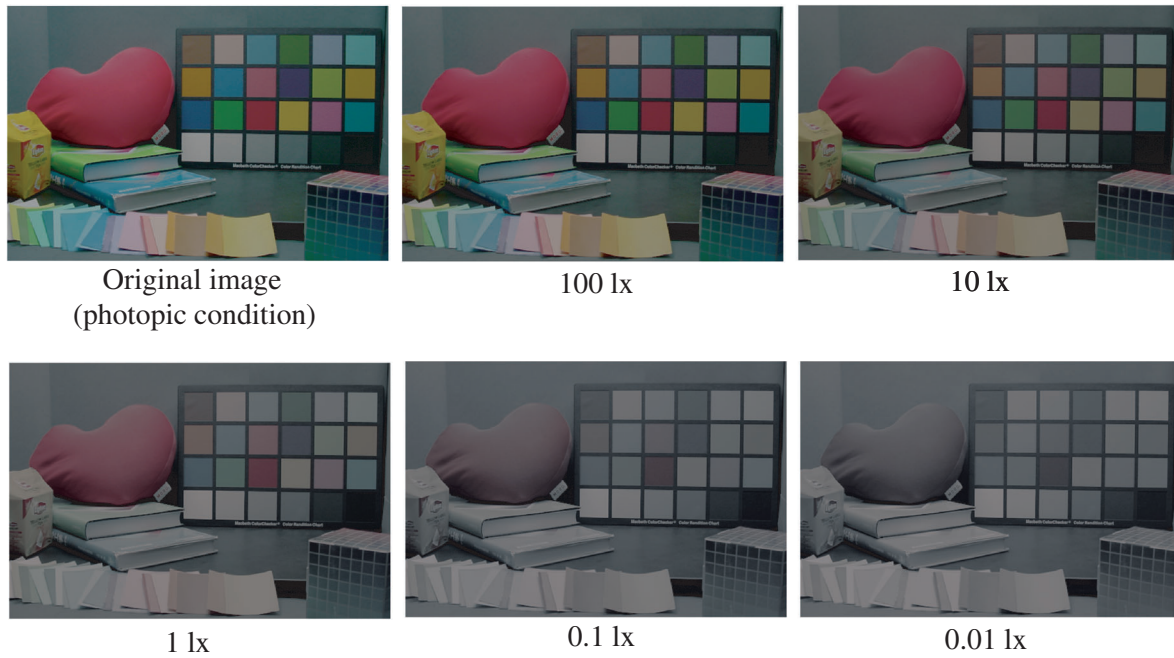


Fig. 7. Simulation results of an image (the image at 1000 lx is the original) at five different illuminance levels.

$$\therefore \begin{pmatrix} R \\ G \\ B \end{pmatrix} = \begin{pmatrix} 0.73179 & -0.31367 & -0.11155 \\ -0.73769 & 1.33321 & 0.00991 \\ 0.00589 & -0.01954 & 0.10163 \end{pmatrix} \times \begin{pmatrix} X_{\text{Judd}} \\ Y_{\text{Judd}} \\ Z_{\text{Judd}} \end{pmatrix} \quad (13)$$

From the Judd modified  $XYZ$  tristimulus values, the present model simulates outputs of the opponent channel at a illuminance level, which in turn are transformed to the Judd modified  $XYZ$  tristimulus values. Finally, these Judd modified  $XYZ$  tristimulus values provide  $R$ ,  $G$  and  $B$  with the luminance unit for each pixel. Figure 7 shows the original and simulation images at five different illuminance levels.

## 5. Conclusions

We propose a mesopic color appearance model based on a two-stage color model. The model is described in the color space which corresponds to three opponent channels. To predict mesopic color vision, the model has rod signals in each of the opponent channels. It successfully predicts that chromatic component decreases with decrease in illumi-

nance, hue changes with decrease in illuminance similarly to the experimental results, color is perceived even at the illuminance of 0.01 lx and lightness changes differently for bluish and reddish chips as predicted from the Purkinje shift.

## References

- 1) G. Wyszecki and W. Stiles: *Color Science: Concepts and Methods, Quantitative Data and Formulae* (Wiley, New York, 1982) 2nd ed., pp. 451 and 633.
- 2) R. M. Boynton and P. K. Kaiser: *Human Color Vision* (J. Opt. Soc. Am. 1996) 2nd ed., p. 249.
- 3) L. M. Hurvich: *Color Vision* (Sinauer Associates, Massachusetts, 1981) Chap 11.
- 4) R. L. DeValois and K. K. DeValois: *Vision Res.* **33** (1993) 1053.
- 5) S. L. Guth: *J. Opt. Soc. Am.* **A8** (1991) 976.
- 6) R. W. G. Hunt: *The Reproduction of Colour* (Fountain Pr., England, 1995) 5th ed., Chap. 31, p. 705.
- 7) M. D. Fairchild: *Color Appearance Models* (Addison-Wesley, 1998) p. 245.
- 8) S. L. Buck, R. F. Knight and J. Bechtold: *Vision Res.* **40** (2000) 3333.
- 9) J. C. Shin, N. Matsuki, K. Kikuchi, H. Yaguchi and S. Shioiri: AIC, Bangkok, 2003, p. 199.
- 10) J. C. Shin, N. Matsuki, H. Yaguchi and S. Shioiri: Eleventh Color Imaging Conf., Color Science and Engineering Systems, Technologies, Applications, Scottsdale, 2003. p. 165.
- 11) J. C. Shin, H. Yaguchi and S. Shioiri: to be published in *Opt. Rev.*
- 12) V. C. Smith and J. Pokorny: *Vision Res.* **15** (1975) 161.